JCTC Journal of Chemical Theory and Computation

Article

pubs.acs.org/JCTC

Attenuated MP2 with a Long-Range Dispersion Correction for Treating Nonbonded Interactions

Matthew B. Goldey,[†,‡,¶] Bastien Belzunces,[†,§] and Martin Head-Gordon*[,†,‡]

[†]Kenneth S. Pitzer Center for Theoretical Chemistry, Department of Chemistry, University of California, Berkeley, California 94720, United States

[‡]Chemical Sciences Division, Lawrence Berkeley National Laboratory, Berkeley, California 94720, United States

Supporting Information

ABSTRACT: Attenuated second order Møller−Plesset theory (MP2) captures intermolecular binding energies at equilibrium geometries with high fidelity with respect to reference methods, yet must fail to reproduce dispersion energies at stretched geometries due to the removal of fully long-range dispersion. For this problem to be ameliorated, long-range correction using the VV10 van der Waals density functional is added to attenuated MP2, capturing short-range correlation with attenuated MP2 and long-range dispersion with VV10. Attenuated MP2 with long-range VV10 dispersion in the aug-cc-pVTZ (aTZ) basis set, MP2-V(terfc, aTZ), is parametrized for noncovalent interactions using the S66 database and tested on a variety of noncovalent databases, describing potential energy surfaces and equilibrium binding energies equally well. Further, a spin-component scaled (SCS) version, SCS-MP2-V(2terfc, aTZ), is produced using the W4-11 database as a supplemental thermochemistry training set, and the resulting method reproduces the quality of MP2-V(terfc, aTZ) for noncovalent interactions and exceeds the performance of SCS-MP2/aTZ for thermochemistry.

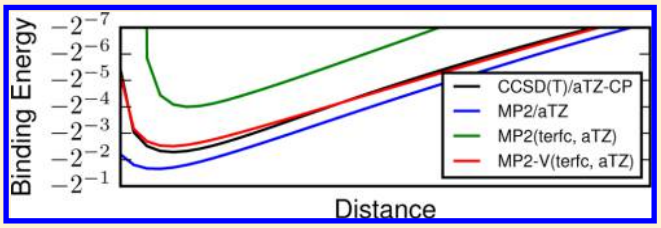

1. INTRODUCTION

Modeling chemical problems requires a choice of theory and basis set,[1] which requires consideration of the inherent accuracy of a method, the underlying cost, and the limitations of a given finite basis set. Second-order Møller−Plesset perturbation theory (MP2)[2,3] provides an excellent compromise between accuracy and feasibility for problems that include water clusters[4,5] and ion−water interactions.[6,7] Unlike hydrogen-bonded systems, other long-range noncovalent interactions are normally poorly treated by MP2, often through overbinding.[8−11] This behavior comes from inaccurate long-range C_6 coefficients describing the treatment of dispersion within MP2.[12,13] As is well-known, the MP2 correlation energy converges slowly to the complete basis set (CBS) limit with increases in the size of the atomic orbital basis set,[14] which causes challenges in applications such as conformational analysis.[15]

Because of its relatively low cost ($O(N^5)$ scaling with system size) compared to more quantitative theories, many attempts have been made to improve the accuracy of MP2 through the use of semiempirical corrections, including scaling the correlation energy[16,17] and scaling the opposite-spin (OS) and same-spin (SS) components of the MP2 correlation energy (spin-component scaled MP2, SCS-MP2).[18−20]

$$E_{\text{SCS-MP2}} = c_{\text{OS}}E_{\text{OS}} + c_{\text{SS}}E_{\text{SS}} \tag{1}$$

Such methods have made significant improvements in the treatment of covalently bonded systems and more moderate improvements for noncovalent interactions.[21−24] The optimal scaling coefficients are significantly different for bonded versus nonbonded interactions.[20]

Density functional theory (DFT), at least in its standard semilocal forms that depend only on properties of the density at a given location, is well-known to omit long-range dispersion interactions.[25] Much work has been done to reincorporate missing long-range dispersion with considerable success. Simple approximations of the dispersion interaction through pairwise precomputed C_6 values have exchanged qualitative failure for a frequently useful level of accuracy for noncovalent interactions.[26−29] Other methods of computing C_6 coefficients using properties like the exchange-dipole moment[30] or the Hirshfeld volumes of atoms[31] have proven similarly successful. An alternative approach relying upon finding functionals of the density at more than one location has produced the van der Waals (vdW) density functionals, both in parameterless and parametrized[32−36] forms. vdW functionals cast dispersion in terms of the interaction of the density at two points, mediated by a local approximation to the dynamic polarizability (Φ).

$$E_{\text{nl}}^{c} = \int \mathrm{d}\mathbf{r}\rho(\mathbf{r}) \int \mathrm{d}\mathbf{r}'\rho(\mathbf{r}')\Phi(|\mathbf{r} - \mathbf{r}'|) \tag{2}$$

Self-consistently training vdW functionals as part of a density functional has recently led to functionals such as ωB97X-V[37] and B97M-V[38] that are very accurate for noncovalent interactions. However, unlike wave function methods, they

Received: May 29, 2015
Published: August 3, 2015

DOI: 10.1021/acs.jctc.5b00509
J. Chem. Theory Comput. 2015, 11, 4159−4168

still suffer from self-interaction errors[39,40] due to incomplete use of exact exchange.

Using a different approach, we have recently addressed the inadequacies of MP2 for noncovalent interactions. By introducing range-separation into the Coulomb operator, a short-range, or "attenuated", MP2 method[41] is produced that preserves only short-range electron correlation. The resulting attenuated MP2 method reduces errors of MP2 in a given basis set by as much as a factor of 5.[41] This is achieved because attenuation partially cancels the inherent overbinding of MP2 and the additional overbinding due to basis set superposition error (BSSE) in finite basis sets. The full Coulomb operator is retained for the underlying Hartree−Fock (HF) calculation. Using one range-separation parameter, r_0, attenuated MP2 has been parametrized for the aug-cc-pVDZ[41] and aug-cc-pVTZ[42] Dunning basis sets[43,44] and other basis sets.[45] Tests on large systems were also reported.[46] Attenuated MP2 was extended to benefit bonded interactions at the same time as nonbonded interactions by incorporating spin-component scaling into a range-separation ansatz to define the SCS-MP2(2terfc, aTZ) method.[47] SCS-MP2(2terfc, aTZ) captures the behavior of MP2(terfc, aTZ) for noncovalent interactions while reproducing SCS-MP2/aTZ for thermochemistry databases.

Despite these successes, purely dispersive interactions are missing from the treatment of long-range interactions within attenuated MP2. Indeed, the long-range C_6 coefficients are zero for attenuated MP2. To address this issue, we paired further modifications of attenuated MP2 with the long-range dispersion energy from time-dependent Kohn−Sham (TD-KS) density functional theory to form the attenuated MP2C method,[48] which approximates the full MP2C energy[49] within a much smaller basis than is needed to converge the MP2C/CBS values. MP2C requires clearly separable fragments, which is true for intermolecular interactions, including molecular crystals, but is not satisfied for other important nonbonded interactions, such as intramolecular conformational analysis. Still, the success in pairing attenuated MP2 with the TD-KS polarizabilities suggests that attenuated MP2 is potentially compatible with long-range corrections.

It is also worth noting that even though all long-range two-electron integrals are neglected, attenuated MP2 quantitatively captures the leading long-range correlation effects for systems with nonzero dipole moments, such as the water dimer. The reason is that mean-field HF yields incorrect electrical moments, which are corrected by MP2. The resulting dipole moment corrections give a long-range R^{-3} dependence for the correlation binding energy in the water dimer. Attenuated MP2 captures this correctly, regardless of its neglect of long-range dispersion.[50] For this reason, a VV10 correction to HF is unpromising (it cannot correct the errors in long-range HF electrostatics), but a VV10 correction to MP2 is quite promising, as it can potentially reincorporate long-range dispersion.

In the remainder of this paper, we pursue that goal by combining attenuated MP2 with long-range VV10 correlation to define a method that correctly includes long-range dispersion and then carefully assess its performance against conventional MP2 and the existing (uncorrected) attenuated MP2 methods.

2. METHODS

Attenuated MP2 partitions the Coulomb operator into short- and long-range components using the terf switching function,[51] which depends on a single parameter, r_0.

$$\mathrm{terf}(r, r_0) = \frac{1}{2}\left(\mathrm{erf}\left[\frac{(r - r_0)}{r_0\sqrt{2}}\right] + \mathrm{erf}\left[\frac{(r + r_0)}{r_0\sqrt{2}}\right]\right) \tag{3}$$

$$\frac{1}{r} = \frac{\mathrm{terf}(r, r_0)}{r} + \frac{\mathrm{terfc}(r, r_0)}{r} \tag{4}$$

The short-range function, $\frac{\mathrm{terfc}(r, r_0)}{r}$ is equivalent to a shifted $\frac{1}{r}$ at $r = 0$ because the first and second derivatives of the corresponding long-range Coulomb operator, $\frac{\mathrm{dterf}(r, r_0)}{\mathrm{d}r}$ and $\frac{\mathrm{d}^2\mathrm{terf}(r, r_0)}{\mathrm{d}r^2}$, are zero at the origin by design.

The attenuated MP2 correlation energy uses a modified Coulomb operator employing the complementary terf function (terfc), resulting in an energy expression that involves attenuated integrals. In terms of spin-orbitals, attenuated MP2 is

$$E_{\mathrm{MP2}} = -\frac{1}{2} \sum_{ij}\sum_{ab} \frac{\left(ia\left|\frac{\mathrm{terfc}(r_{12}, r_0)}{r_{12}}\right|jb\right)\left[\left(ia\left|\frac{\mathrm{terfc}(r_{12}, r_0)}{r_{12}}\right|jb\right) - \left(ib\left|\frac{\mathrm{terfc}(r_{12}, r_0)}{r_{12}}\right|ja\right)\right]}{\epsilon_a + \epsilon_b - \epsilon_i - \epsilon_j} \tag{5}$$

The range-separation of the MP2 correlation energy is analogous to using two perturbations corresponding to the short- and long-range fluctuation potential. These two perturbations give rise to three energetic terms at second order, purely short-range correlation (SR), purely long-range correlation (LR), and mixed-range correlation (MR). The MR term is linear in each of the two perturbations.

$$E_{\mathrm{MP2}} = E_{\mathrm{SR}} + E_{\mathrm{MR}} + E_{\mathrm{LR}} \tag{6}$$

These terms sum to the full MP2 correlation energy regardless of the range-separation distance. Attenuated MP2 corresponds to the neglect of the second and third terms, motivated by the known overbinding of MP2 at the CBS limit, which is further increased by basis set superposition errors.

To consider how one might couple attenuated MP2 with a long-range correction, let us first examine the asymptotic decay of attenuated MP2 itself. This is given by expanding the attenuated MP2 energy for two nonoverlapping closed shell subunits, A and B, in a manner similar to that of Szabo and Ostlund[12] for occupied (virtual) molecular orbitals i,j (a,b) with superscripts indicating the fragment and $\tilde{\ }$ denoting the modified integrals.

$$\Delta E_{\mathrm{MP2}}^{(\mathrm{A-B})} = E_{\mathrm{MP2}}^{(\mathrm{A})} + E_{\mathrm{MP2}}^{(\mathrm{B})} + 4\frac{|(i^{(\mathrm{A})}a^{(\mathrm{A})}|\tilde{j}^{(\mathrm{B})}b^{(\mathrm{B})})|^2}{\epsilon_{i^{(\mathrm{A})}} + \epsilon_{j^{(\mathrm{B})}} - \epsilon_{a^{(\mathrm{A})}} - \epsilon_{b^{(\mathrm{B})}}} \tag{7}$$

The Coulomb operator is expanded around the intermolecular separation, $\mathbf{R}$, with local position operators, ${}^{\mathrm{A}}\mathbf{r}_1$ and ${}^{\mathrm{B}}\mathbf{r}_2$.

$$\frac{1}{|\mathbf{r}_{12}|} = \frac{1}{|{}^{\mathrm{A}}\mathbf{r}_1 - {}^{\mathrm{B}}\mathbf{r}_2 - \mathbf{R}|} = \frac{1}{|\mathbf{R}|} + \frac{{}^{\mathrm{A}}\mathbf{x}_1\cdot{}^{\mathrm{B}}\mathbf{x}_2 + {}^{\mathrm{A}}\mathbf{y}_1\cdot{}^{\mathrm{B}}\mathbf{y}_2 - 2\,{}^{\mathrm{A}}\mathbf{z}_1\cdot{}^{\mathrm{B}}\mathbf{z}_2}{|\mathbf{R}|^3} + \ldots \tag{8}$$

The attenuated Coulomb operator will have a very similar expansion, where we truncate the expansion for $\mathrm{terfc}(|\mathbf{r}_{12}|, r_0)$ at $\mathbf{R} = \mathbf{r}_{12}$ given the very weak dependence on $\mathbf{r}_{12}$ at large separation with our range-separation function.

DOI: 10.1021/acs.jctc.5b00509
J. Chem. Theory Comput. 2015, 11, 4159−4168

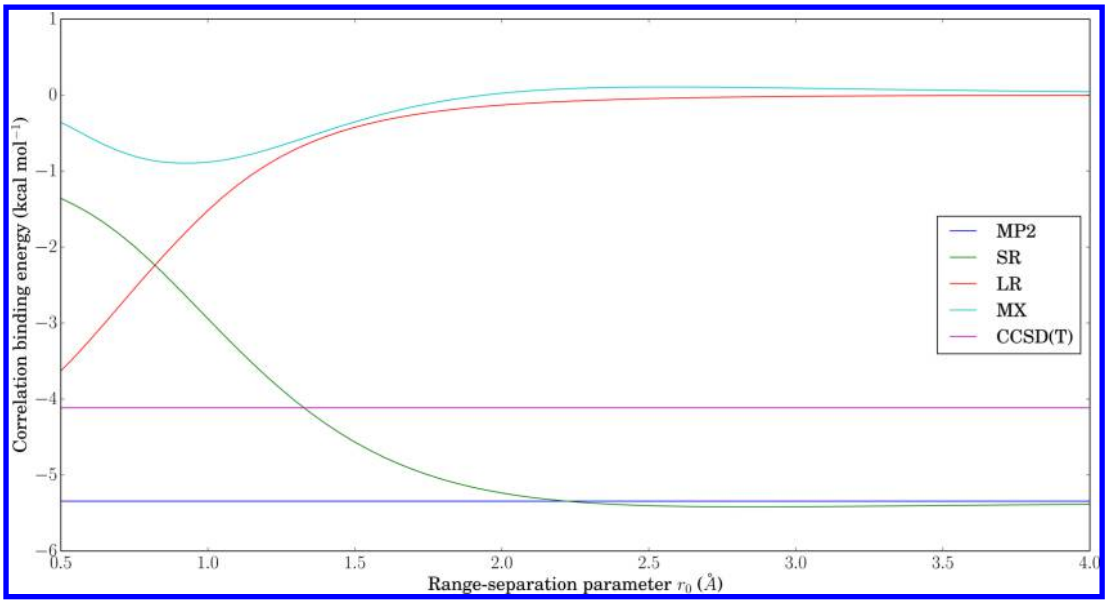

Figure 1. Average correlation binding energy versus range-separation parameter r_0 on the S66 database for MP2/aTZ (MP2), MP2(terfc, aTZ) (SR), long-range MP2 (LR), and the mixed short−long-range correlation (MX). For reference, the average CCSD(T)/CBS binding energies are also presented (CCSD(T)) with HF/aTZ binding energies removed to present the correlation binding energy on the same scale.

$$\frac{\mathrm{terfc}(|\mathbf{r}_{12}|, r_0)}{|\mathbf{r}_{12}|} = \mathrm{terfc}(|\mathbf{R}|, r_0) \left[\frac{1}{|\mathbf{R}|} + \frac{{}^{A}\mathbf{x}_1 \cdot {}^{B}\mathbf{x}_2 + {}^{A}\mathbf{y}_1 \cdot {}^{B}\mathbf{y}_2 - 2\,{}^{A}\mathbf{z}_1 \cdot {}^{B}\mathbf{z}_2}{|\mathbf{R}|^3} + \ldots\right] + \ldots \quad (9)$$

The resulting dispersion energy within attenuated MP2 is then given by the MP2(uncoupled Hartree−Fock)-level C_6 coefficients, which are strongly damped by terfc(R,r_0)^2.

$$E_{\mathrm{disp.}}^{\mathrm{att.\,MP2}} = -(\mathrm{terfc}(R, r_0))^2 \frac{C_6^{\mathrm{MP2}}}{R^6} \quad (10)$$

This necessarily fails to capture the dispersion interactions, which is the motivation for this manuscript.

A numerical test of the magnitude of the SR, MR, and LR contributions is given in Figure 1, which shows the average correlation binding energy of range-separated MP2 for the S66 database.[52] This figure indicates that the majority of the correlation binding energy is recovered by MP2(terfc, aTZ) for range-separation parameters larger than 0.95 Å. At the parameter used for MP2(terfc, aTZ) (1.35 Å), the average long-range and mixed correlation binding energies for this database are −0.62 and −0.54 kcal mol^{-1}, relative to the SR term, which is around −4 kcal/mol. Because both the MR and LR terms involve the long-range perturbation, which is contaminated with BSSE and incorrect C_6 values, we choose to replace them together with a good long-range correction, as we shall now discuss.

As a natural complement to the truncation of the electron−electron interaction within attenuated MP2, the van der Waals density functionals also depend upon the interelectron separation of two electron densities. In this work, we have used the VV10 density functional.[35] In addition to the inherent damping included in the model, further removal of electron−electron correlation is necessary to avoid double-counting short-range correlation. An additional multiplicative damping function, $1 - \mathrm{terfc}(r_{12},r_0)^2$, is used to remove short-range portions of the VV10 correlation energy that are redundant with what is retained in attenuated MP2. Thus, we use VV10 modified as follows

$$E_{\mathrm{nl}}^{c} = \int \mathrm{d}\mathbf{r}\rho(\mathbf{r}) \int \mathrm{d}\mathbf{r}'\rho(\mathbf{r}')\Phi_{\mathrm{VV10}}(|\mathbf{r} - \mathbf{r}'|, b, C)(1 - \mathrm{terfc}(|\mathbf{r} - \mathbf{r}'|, r_0)^2) \quad (11)$$

The r_0 parameter is shared with the attenuated short-range MP2 part rather than being adjusted separately. The VV10 kernel, Φ_{VV10}, depends on two semiempirical parameters, b, which controls the strength of short-range damping, and C, which controls the magnitude of C_6 coefficients.

This work uses a developmental version of Q-Chem 4.2[53] for all energies not from the literature. MP2 values reported herein use the resolution of the identity approximation (RI)[54] when RI basis sets were available for the substituent atoms. The frozen core approximation was used for all wave function results reported. Grid-based VV10 calculations use the SG1 grid, except in cases of SCF convergence problems. Counterpoise corrections were not performed unless otherwise indicated. Complete basis set estimates of MP2 and CCSD(T) binding energies have been used from the appropriate references when databases are used.

3. TRAINING

The dispersion corrected attenuated MP2 method is semiempirical because it depends upon several parameters that are nonlinear: first, r_0, which is associated with attenuating short-range correlation in eq 5; next, the two VV10 parameters b and C, and finally, the choice of the finite basis set that will be employed. Because our previous work on attenuated MP2 achieved the greatest success with the Dunning aug-cc-pVTZ (aTZ) basis, we shall use it again here. We chose to fix the long-range correlation parameter C at the value optimized for LC-VV10 (long-range corrected VV10), namely, C = 0.0089. This choice ensures high-quality long-range C_6 values. The remaining two parameters will be sampled on a 2-dimensional grid. The resulting van der Waals corrected attenuated MP2 method will be denoted as MP2-V(terfc, aTZ) to indicate its choice of attenuating function (terfc) and the chosen aTZ basis.

DOI: 10.1021/acs.jctc.5b00509
J. Chem. Theory Comput. 2015, 11, 4159−4168

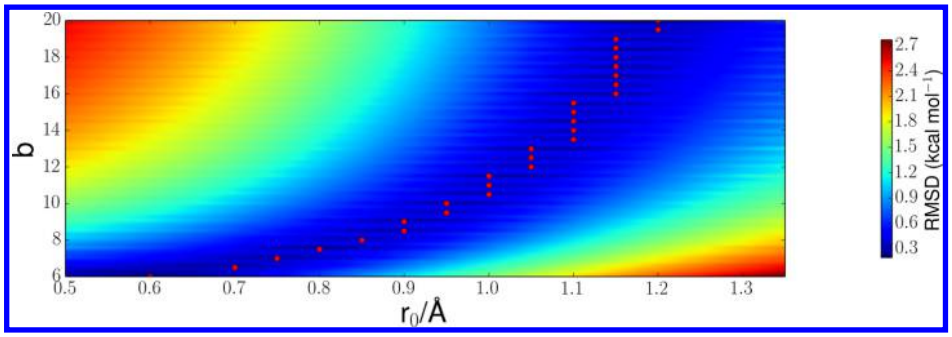

Figure 2. Root-mean-square deviation (kcal mol^{-1}) on the 66 intermolecular interactions of the S66 data set versus r_0/Å and b for MP2-V(terfc, aTZ) with optimal r_0 for each b denoted in red as an aid to the reader. Note that data points were taken in units of 0.05 Å for r_0 and in units of 0.5 for b, and an interpolation grid of 75 points in each direction was used for this graphic.

A database must be used to train the parameters, and we chose the S66 database[52] due to its variety of noncovalent interactions. S66 contains CCSD(T)/CBS references for small homo and heterodimers of 3−4 atoms as well as larger nucleic acid complexes. Scanning r_0 in units of 0.05 Å and damping parameter b in units of 0.1, we generated nonlocal correlation energies with converged Hartree−Fock densities for the S66 data set in a nonself-consistent manner. The results for MP2-V(terfc, aTZ) on the S66 training set are presented in Figure 2. Recalling that the optimal value for MP2(terfc, aTZ) was r_0 = 1.35 Å, it is evident that stronger attenuation (i.e., smaller r_0) is possible in the VV10-corrected model. A range of possible r_0 values between approximately 0.8 and 1.2 Å appear to be viable with the preferred value of b increasing strongly (i.e., stronger damping) as r_0 increases (i.e., weaker attenuation).

Self-consistent usage of the VV10 nonlocal correlation is presented in Table 1 using the optimal b parameter for each r_0 near the minimum of our objective function (here, root-mean-square deviation, RMSD). The optimal parameters for MP2-V(terfc, aTZ) generate an RMSD on this data set of 0.199 kcal mol^{-1}, which is essentially identical to the non-self-consistent value of 0.202 kcal mol^{-1}. Hence, VV10 can be used as a post-HF correction if desired. The optimal damping parameter b is found to be 11.0, somewhat larger than the b = 6.9 chosen for LC-VV10 despite our additional short-range damping of the VV10 correlation energy, suggesting that the short-range correlation energy within attenuated MP2 describes correlation over a wider spatial extent than that described by the PBE correlation energy used by the VV10 functionals. The optimal r_0 for MP2-V(terfc, aTZ), 1.00 Å, is substantially shorter than for MP2(terfc, aTZ) at 1.35 Å, which is potentially advantageous for future efficient implementation of the short-range MP2 part. MP2-V(terfc, aTZ) possesses the correct long-range limit by design.

Table 1. Overall Root-Mean-Square Deviation (RMSD), RMSD for the Hydrogen-Bonded (HB), Dispersion-Bonded (DISP), and Mixed Interactions (MIX) Subsets, as well as Mean-Signed Error (MSE) and Mean-Unsigned Error (MUE) on the S66 Database in kcal mol^{-1} for MP2-V(terfc, aTZ) with Self-Consistent Orbitals Using HF Plus VV10 As Computed with the Optimal b Value for Various r_0 Values Near the Global Minimum

r_0/Å	b	RMSD	HB	DISP	MIX	MSE	MUE
0.85	8.0	0.206	0.182	0.204	0.232	−0.043	0.172
0.90	9.0	0.200	0.180	0.208	0.212	0.015	0.169
0.95	9.5	0.212	0.190	0.201	0.246	−0.077	0.178
1.00	11.0	0.199	0.180	0.195	0.223	−0.019	0.167
1.05	12.5	0.201	0.179	0.197	0.228	−0.024	0.167
1.10	14.5	0.204	0.178	0.202	0.234	−0.026	0.169

We turn next to the training of a spin-component scaled (SCS) version of MP2-V that aims for improved performance on thermochemical properties in addition to nonbonded interactions. For SCS-MP2-V(2terfc, aTZ), we have three more parameters to tune the short-range correlation energy following the SCS-MP2(2terfc, aTZ) method.[47] The method uses short-range OS MP2 correlation (with r_0^{SR}) and a midrange SS MP2 correlation constructed from the difference between the SS correlation at r_0^{MR} and r_0^{SR} as well as separate spin-component scaling parameters, according to

$$E = c_{OS}E_{OS}(r_0^{SR}) + c_{SS}[E_{SS}(r_0^{MR}) - E_{SS}(r_0^{SR})] \quad (12)$$

To have the possibility of improved performance for thermochemistry, it is essential to train the parameters on both the nonbonded interactions of the S66 database and additional bonded interactions. For the latter purpose, we employ the W4-11 database of thermochemical reactions.[55] To place the nonbonded and bonded interactions on a more-or-less equal footing in the optimization process, we define a figure of merit that is a weighted average of the RMS errors in the two data sets

$$\mathrm{RMSD}_{\mathrm{Weighted}} = \frac{|E|_{\mathrm{W4\text{-}11}}\mathrm{RMSD}_{\mathrm{S66}} + |E|_{\mathrm{S66}}\mathrm{RMSD}_{\mathrm{W4\text{-}11}}}{|E|_{\mathrm{W4\text{-}11}} + |E|_{\mathrm{S66}}} \quad (13)$$

The quantities $|E|_{W4\text{-}11}$ and $|E|_{S66}$ are the average magnitude of the interaction energy in each of the two databases.

We present a slice of the resulting parameter search in Figure 3, where we scan the short- and midrange r_0 values (choosing the optimal same- and opposite-spin scaling coefficients and damping parameter b at each point). Enforcing a minimum difference of 0.2 Å between the attenuation parameters, we find an optimal b of 14.0, and optimal short- and midrange attenuation parameters of 0.70 and 0.90 Å. The attenuation parameters are contracted compared to the SCS-MP2(2terfc, aTZ) values of 0.75 and 1.05 Å, though to a lesser degree than in MP2-V because these are already quite short-ranged. Because the midrange correlation is the most extended correlation under consideration, the corresponding midrange attenuation parameter is used in enhancing the damping function of the VV10 correlation energy. The spin-component scaling coefficients c_{OS} and c_{SS} are 1.267 and 4.444, respectively,

DOI: 10.1021/acs.jctc.5b00509
J. Chem. Theory Comput. 2015, 11, 4159−4168

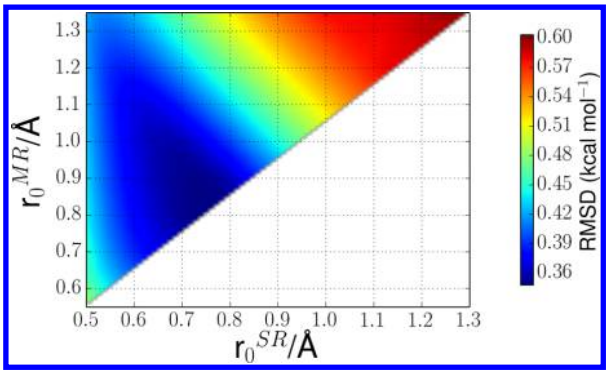

Figure 3. Root-mean-square deviation (kcal mol^{-1}) on the 66 intermolecular interactions of the S66 data set versus r_0/Å and b for SCS-MP2-V(2terfc, aTZ). Note that data points were taken in units of 0.05 Å for r_0^{SR} and r_0^{MR} and in units of 0.5 for b, and the linear parameters c_{OS} and c_{SS} are fitted at each point. An interpolation grid of 75 points in each direction was used for this graphic. Note that the method is only defined for $r_0^{MR} > r_0^{SR}$, and therefore, only half the grid is populated with values.

which are similar to those without dispersion correction (1.27 and 4.05).

The behavior of the new van der Waals corrected methods versus existing methods for intermolecular interaction energies on the S66 training set is summarized in Table 2, along with MP2/aTZ and MP2/CBS results. There is a useful 20% reduction in the RMS error between MP2(terfc, aTZ) and MP2-V(terfc, aTZ), which accompanies the improved physical content (correct long-range behavior). The RMS error reduction is closer to 10% between SCS-MP2(terfc, aTZ) and SCS-MP2-V(terfc, aTZ). Because we are intent on enforcing the correct long-range physics, these improvements suggest that the range-separated treatment of different physics at different regimes is working quite satisfactorily in the training set. It is worth noting that the RMS errors for MP2-V and SCS-MP2-V are over seven times smaller than for MP2 in the same aTZ basis set.

As an additional diagnostic, the interaction type dependence for the S66 database is presented in Figure 4. Subset identification follows that of Řezáč, Riley, and Hobza.[56] Van der Waals correction for these methods consistently improves relative to uncorrected MP2, providing uniform and excellent performance for each of these interaction motifs (all methods with vdW correction have RMSD < 0.25 kcal mol^{-1} for every interaction type). In particular, π-stacking is noticeably improved by the incorporation of either van der Waals correction or spin-component scaling.

The behavior of the new van der Waals corrected attenuated MP2 methods versus existing MP2 methods for thermochemical energies on the W4-11 training set is summarized in Table 3. SCS-MP2-V(2terfc, aTZ) performs quite well on this set with an RMS error of 4.36 kcal mol^{-1}. A 40% reduction in RMS error relative to MP2-V(terfc, aTZ) shows that spin component

Table 2. Root-Mean-Square Deviation (RMSD), Mean-Signed Error (MSE), Mean-Unsigned Error (MUE), and Maximum Error (MAX) on the S66 Database in kcal mol^{-1} for MP2 and Attenuated MP2 in the aug-cc-pVDZ (aDZ) and aug-cc-pVTZ (aTZ) Basis Sets with Spin-Component Scaling and VV10-Corrections Included for Attenuated MP2

method	RMSD	MSE	MUE	MAX
MP2/CBS	0.731	−0.405	0.481	2.205
MP2/aDZ	2.666	−2.151	2.151	6.157
MP2/aTZ	1.533	−1.229	1.229	3.665
MP2(terfc, aDZ)	0.426	0.051	0.325	1.069
MP2(terfc, aTZ)	0.251	−0.068	0.208	0.521
SCS-MP2(2terfc, aTZ)	0.228	−0.015	0.182	0.516
MP2-V(terfc, aTZ)	0.199	−0.019	0.167	0.458
SCS-MP2-V(2terfc, aTZ)	0.194	−0.031	0.163	0.499

Table 3. Root-Mean-Square Deviation (RMSD), Mean-Signed Error (MSE), Mean-Unsigned Error (MUE), and Maximum Error (MAX) on the W4-11 Database in kcal mol^{-1} for Unmodified MP2, Spin-Component Scaled MP2, Attenuated MP2, VV10-Corrected Attenuated MP2, and Spin-Component Scaled VV10-Corrected Attenuated MP2

method	RMSD	MSE	MUE	MAX
MP2/aTZ	7.29	−1.69	5.59	25.73
SCS-MP2/aTZ	5.16	0.10	3.57	22.15
MP2(terfc, aTZ)	6.97	−1.33	5.46	24.34
SCS-MP2(2terfc, aTZ)	4.79	−0.63	3.38	20.09
MP2-V(terfc, aTZ)	7.26	−0.61	5.51	40.18
SCS-MP2-V(2terfc, aTZ)	4.36	−0.12	3.02	32.82

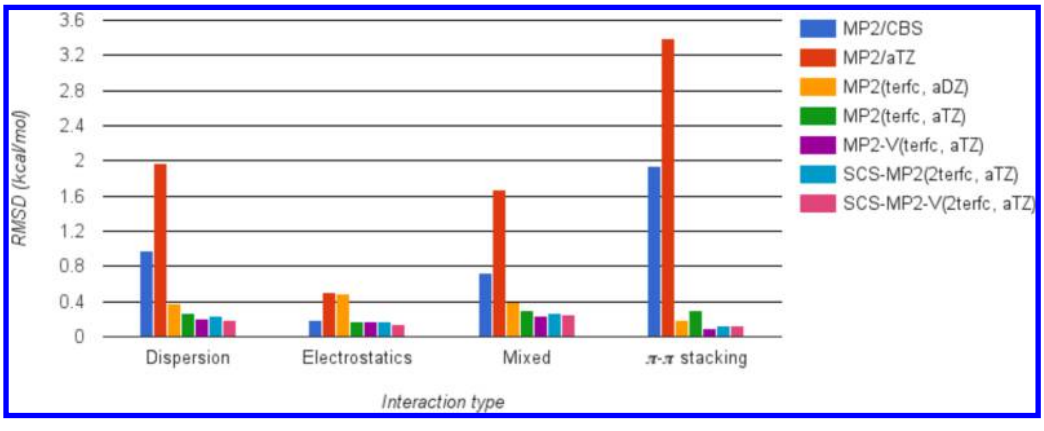

Figure 4. Root-mean-square deviation (RMSD) in kcal mol^{-1} versus interaction type for MP2 at the complete basis set (CBS) limit and in the aug-cc-pVTZ (aTZ) basis and for attenuated MP2 in the aug-cc-pvDZ (aDZ) and aug-cc-pVTZ basis sets. Spin-component scaling and VV10-corrections are included for attenuated MP2.

DOI: 10.1021/acs.jctc.5b00509
J. Chem. Theory Comput. 2015, 11, 4159−4168

scaling is very effective in this application. The roughly 10% RMS error reduction over SCS-MP2(2terfc, aTZ) is in agreement with observations in the literature that dispersion correction can improve statistical behavior for thermochemistry.[57] The mean-signed error for SCS-MP2-V(2terfc, aTZ) is also comparatively low (−0.12 kcal mol^{-1}). MP2-V(terfc, aTZ) performs comparatively poorly with an RMS error of 7.26 kcal mol^{-1}, which is roughly the same as that of unmodified MP2 (7.29 kcal mol^{-1}) and (very) slightly poorer than the original MP2(terfc, aTZ) method.

4. TRANSFERABILITY TESTS

Critical tests of the transferability of these van der Waals corrected methods are the potential energy surfaces corresponding to the S66 set of dimers. CCSD(T)/CBS energies for dimer geometries with scaled interfragment distances (S66×8) and angular distortions (S66a8) are available.[56] Error metrics for all of the geometries in the S66×8 database are presented in Table 4. We find that the overall RMSD for attenuated MP2 is reduced by over 30% upon inclusion of the van der Waals correction, from 0.33 to 0.21 kcal mol^{-1}. The spin-component scaling version behaves essentially identically to the unscaled version.

Table 4. Root-Mean-Square Deviation (RMSD), Mean-Signed Error (MSE), Mean-Unsigned Error (MUE), and Maximum Error (MAX) on the S66×8 Database in kcal mol^{-1} for Unmodified MP2, Attenuated MP2, VV10-Corrected Attenuated MP2, and Spin-Component Scaled VV10-Corrected Attenuated MP2

method	RMSD	MSE	MUE	MAX
MP2/aTZ	1.348	−0.947	0.947	5.403
MP2(terfc, aTZ)	0.325	−0.039	0.236	1.527
MP2-V(terfc, aTZ)	0.207	−0.062	0.151	1.021
SCS-MP2-V(2terfc, aTZ)	0.209	−0.059	0.151	0.917

For further insight, we turn to the RMSD for the different subsets of the S66×8 database separated according to the factor scaling the equilibrium intermolecular separation. The resulting data are presented in Table 5. MP2(terfc, aTZ) performs better than MP2/aTZ for each scaling value of the intermolecular separation. This behavior likely comes from the fact that the long-range electrostatics remain correct at the MP2 level even under attenuation. However, a strong hint of the need for long-range dispersion comes from the fact that while the MP2/aTZ RMSD decreases monotonically with scale factor, attenuated MP2 exhibits a secondary maximum in its RMSD at a scale factor of 1.25.

Table 5. Root-Mean-Square Deviation (RMSD) as a Function of Scaled Intermolecular Distance for the S66×8 Database for Unmodified MP2, Attenuated MP2, VV10-Corrected Attenuated MP2, and Spin-Component Scaled VV10-Corrected Attenuated MP2

scale factor	MP2/aTZ	MP2(terfc, aTZ)	MP2-V(terfc, aTZ)	SCS-MP2-V(2terfc, aTZ)
0.90	2.248	0.627	0.365	0.388
0.95	1.861	0.401	0.279	0.266
1.00	1.610	0.276	0.233	0.213
1.05	1.336	0.228	0.192	0.192
1.10	1.134	0.225	0.161	0.177
1.25	0.753	0.254	0.110	0.129
1.50	0.396	0.213	0.081	0.063
2.00	0.149	0.108	0.053	0.040

By comparison with attenuated MP2, the results for MP2-V(terfc, aTZ) and SCS-MP2-V(2terfc, aTZ) shown in Table 5 are very encouraging for two reasons. Focusing on MP2-V(terfc, aTZ) for concreteness, it is evident first that the RMSD is lower at all scale factors than for MP2(terfc, aTZ) and the improvement increases strongly in percentage terms at larger scale factors where the van der Waals correction should be relatively more important. The reduction in RMSD is over 50% at a scale factor of 1.25 and larger. Second, in contrast to MP2, the RMSD decreases monotonically with scale factor, indicating the effectiveness of the van der Waals correction. The results for SCS-MP2-V(2terfc, aTZ) are similar.

Table 6 presents the results for the S66a8 database.[56] This database contains CCSD(T)/CBS interaction energies for angular displacements of molecules in the S66 database away from equilibrium. Here, MP2-V(terfc, aTZ), with and without spin-component scaling, achieves very low RMS error (0.15 kcal mol^{-1}) with respect to the benchmark values. MP2(terfc, aTZ) without dispersion correction also performs very well (0.21 kcal mol^{-1}) in contrast to MP2/aTZ (1.10 kcal mol^{-1}). Relatively modest improvement is expected for the van der Waals corrected method when applied close to the equilibrium geometries used for parametrizing attenuated MP2.

Table 6. Root-Mean-Square Deviation (RMSD), Mean-Signed Error (MSE), Mean-Unsigned Error (MUE), and Maximum Error (MAX) on the S66a8 Database in kcal mol^{-1} for Unmodified MP2, Attenuated MP2, VV10-Corrected Attenuated MP2, and Spin-Component Scaled VV10-Corrected Attenuated MP2

method	RMSD	MSE	MUE	MAX
MP2/aTZ	1.092	−0.915	0.915	2.815
MP2(terfc, aTZ)	0.209	0.028	0.172	0.514
MP2-V(terfc, aTZ)	0.152	−0.019	0.126	0.427
SCS-MP2-V(2terfc, aTZ)	0.155	−0.018	0.131	0.384

The performance of SCS-MP2-V(2terfc, aTZ) and MP2-V(terfc, aTZ) for the S22 database of intermolecular interactions[8,58] is presented in Table 7. The addition of a dispersion correction to MP2(terfc, aTZ) reduces the RMS error on this database by ∼0.18 kcal mol^{-1}, resulting in an RMS error of 0.301 kcal mol^{-1}. This is over a 30% reduction in RMSD relative to attenuated MP2, which again suggests good transferability of the van der Waals correction. The spin-component scaled method performs slightly worse (0.375 kcal

Table 7. Root-Mean-Square Deviation (RMSD), Mean-Signed Error (MSE), Mean-Unsigned Error (MUE), and Maximum Error (MAX) on the S22 Database in kcal mol^{-1} for Unmodified MP2, Attenuated MP2, VV10-Corrected Attenuated MP2, and Spin-Component Scaled VV10-Corrected Attenuated MP2

method	RMSD	MSE	MUE	MAX
MP2/CBS	1.387	−0.838	0.885	3.596
MP2/aTZ	2.321	−1.684	1.684	5.550
MP2(terfc, aTZ)	0.479	−0.256	0.367	1.257
MP2-V(terfc, aTZ)	0.301	−0.114	0.239	0.757
SCS-MP2-V(2terfc, aTZ)	0.375	−0.130	0.285	1.019

DOI: 10.1021/acs.jctc.5b00509
J. Chem. Theory Comput. 2015, 11, 4159−4168

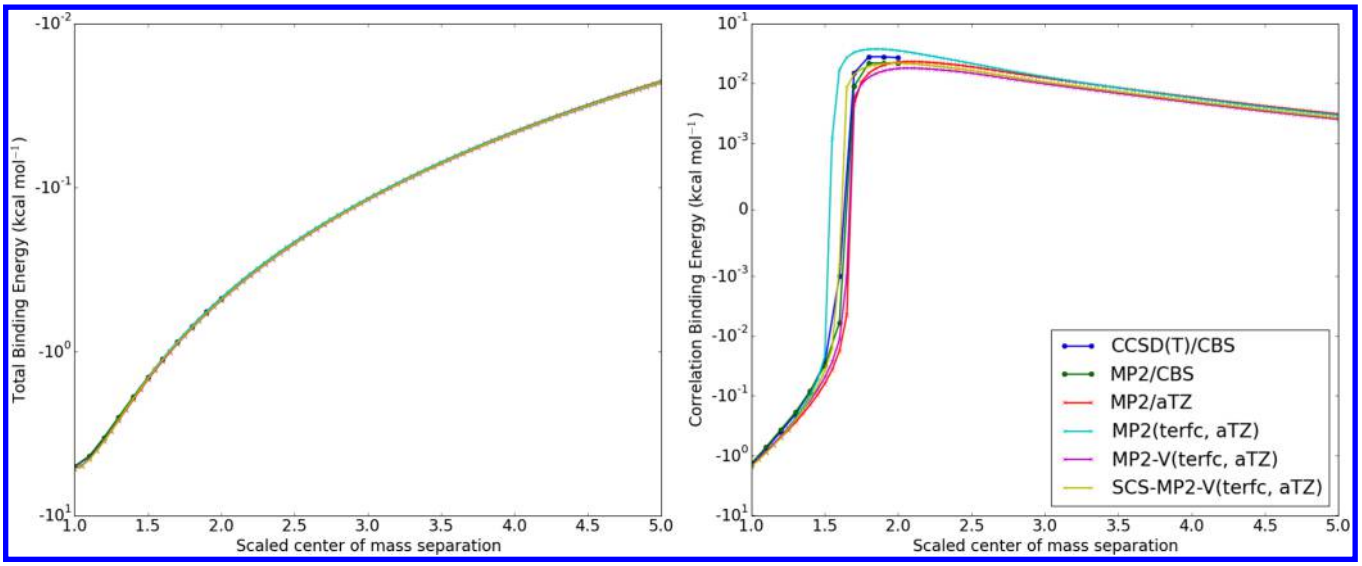

Figure 5. A symmetric log−linear plot of total binding energy (left) and correlation binding energy (right) in kcal mol^{-1} versus scaled center of mass separation for a water dimer. Data points are in increments of 0.05 in scale factor for these figures. Reference results are in increments of 0.1 in scale factor. The *y*-axis is linearized between $\pm 10^{-3}$ kcal mol^{-1}.

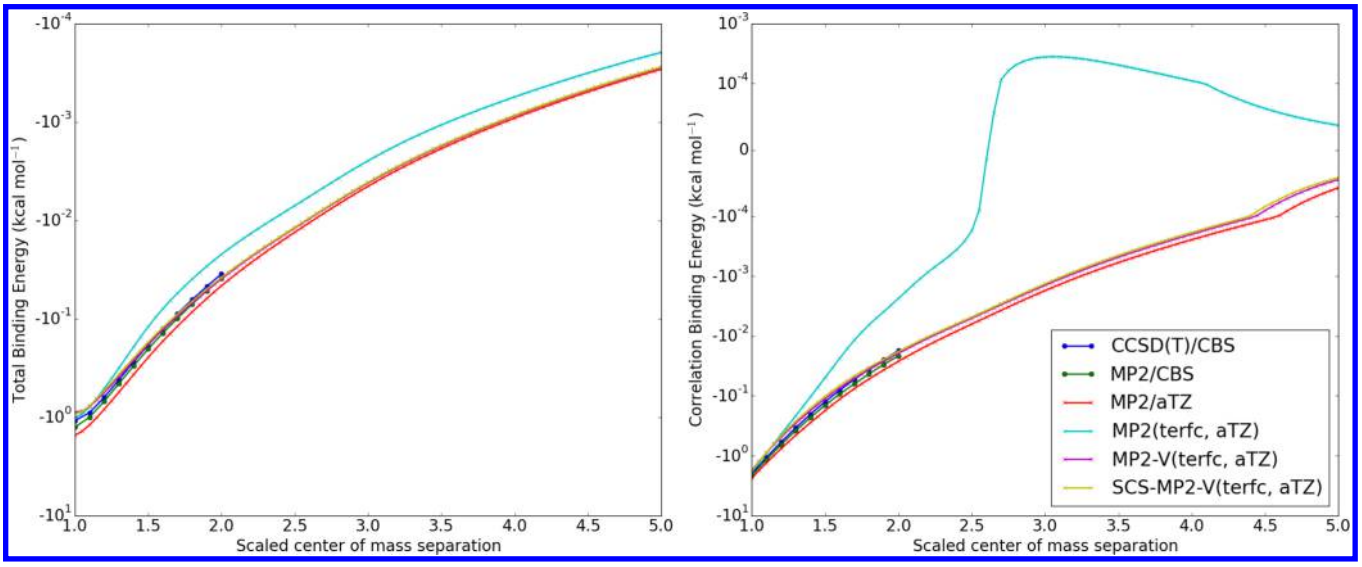

Figure 6. A symmetric log−linear plot of total binding energy (left) and correlation binding energy (right) in kcal mol^{-1} versus scaled center of mass separation for an ethene dimer. Data points are in increments of 0.05 in scale factor for these figures. Reference results are in increments of 0.1 in scale factor. The *y*-axis is linearized between $\pm 10^{-4}$ kcal mol^{-1}. Calculations for this figure used the dual basis approximation.[61,62]

mol^{-1}). The high mean-signed error of MP2/aTZ (−1.684 kcal mol^{-1}) is reduced to ∼ −0.1 kcal mol^{-1} for both MP2-V(terfc, aTZ) and SCS-MP2-V(2terfc, aTZ).

To examine the behavior of attenuated MP2 methods for very stretched potential energy surfaces, performance for the dissociation of three dimers along center of mass coordinates is shown in Figures 5, 6, and 7 for the water dimer, the t-shaped isomer of the ethene dimer, and the argon-methane dimer, which are electrostatically bound, of mixed character, and dispersion-bound, respectively. The equilibrium structures are taken from the A24 database,[59] and the complete basis set (CBS) MP2 and CCSD(T) reference results for the scaled separations are from the A21×12 database[60] (structures and references are available in the Supporting Information).

Very similar behavior is given by attenuated MP2 with and without van der Waals correction for the water dimer in Figure 5 with all of the methods examined, providing a positive correlation binding energy in approximately the same region. This indicates, as noted by Thirman and Head-Gordon,[50] that the long-range correlation energy is dominated by the effect of reducing the HF dipole moment, and thus reducing the attractive dipole−dipole interaction. The long-range VV10 correction makes little visual difference in this case.

The behavior for the ethene dimer, shown in Figure 6, is significantly different. MP2(terfc, aTZ) performs very well at the equilibrium geometry, only to significantly underestimate the total binding energy for separated geometries. The MP2(terfc, aTZ) correlation binding energy serves only to correct inaccurate electrostatics in this system, yielding a positive correlation binding energy at large separations and failing to capture the long-range dispersion interaction. By contrast, MP2-V(terfc, aTZ) and SCS-MP2-V(2terfc, aTZ) both capture long-range dispersion, and the much better

DOI: 10.1021/acs.jctc.5b00509
J. Chem. Theory Comput. 2015, 11, 4159−4168

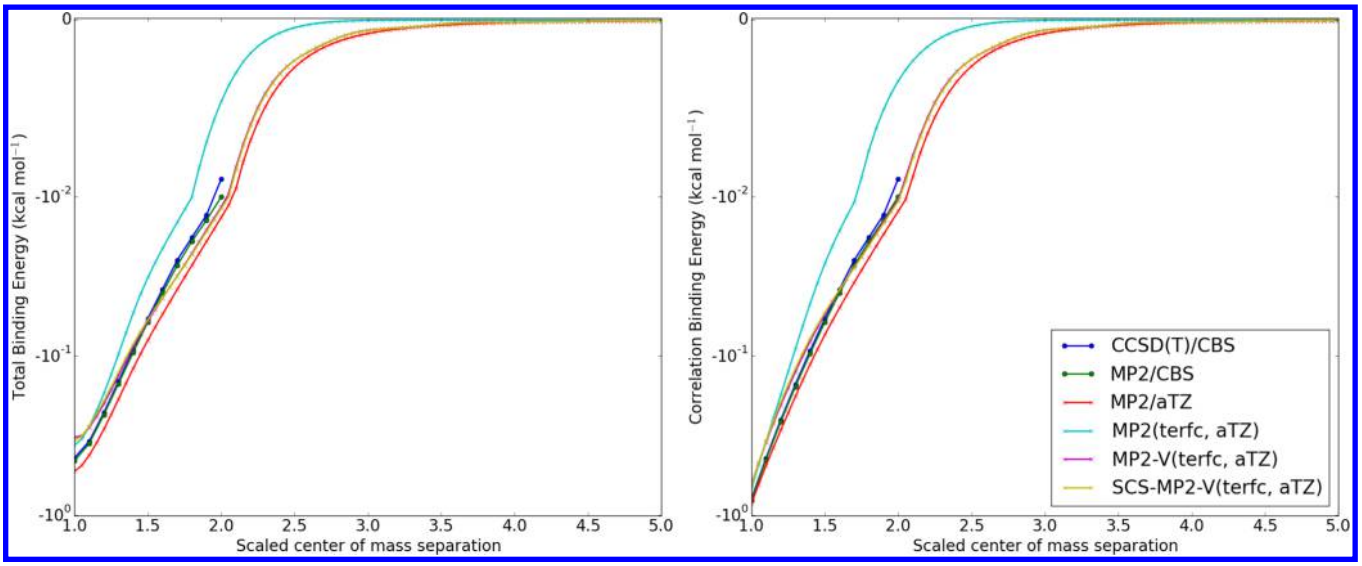

Figure 7. A log−linear plot of total binding energy (left) and correlation binding energy (right) in kcal mol^{-1} versus scaled center of mass separation for an argon-methane dimer. Data points are in increments of 0.05 in scale factor for these figures. Reference results are in increments of 0.1 in scale factor. The *y*-axis is linearized between $\pm 10^{-4}$ kcal mol^{-1}. Calculations for this figure used the dual basis approximation.[61,62]

agreement with the benchmark CCSD(T)/CBS values is graphically evident.

For the purely dispersion-bound argon-methane dimer, shown in Figure 7, the signature of missing dispersion in MP2(terfc, aTZ) is also dramatic with qualitatively different behavior than the benchmark values for both the total binding energy and the correlation binding energy past 1.2 times the equilibrium separation. By contrast, MP2-V(terfc, aTZ) and SCS-MP2-V(2terfc, aTZ) capture this missing dispersion, continuously and differentiably transitioning between a short-range dominated by attenuated MP2 and a long-range dominated by VV10 nonlocal correlation. These examples show the importance of long-range correction in yielding an accurate interaction energy for a range of interfragment separations.

Turning to thermochemistry, the RMSDs obtained by standard and attenuated MP2 methods on the MGAE109[63] and G2/97[64] databases of atomization energies are given in Tables 8 and 9. On the MGAE109 database, SCS-MP2(2terfc, aTZ) and SCS-MP2-V(2terfc, aTZ) perform similarly (RMS errors of ∼5.2 kcal mol^{-1}). These RMS errors are significantly smaller than that obtained with SCS-MP2/aTZ (7.78 kcal mol^{-1}). The improvement of the SCS attenuated MP2 methods over the unscaled attenuated MP2-V(terfc, aTZ) is quite striking (>50% reduction in RMSD) on this database.

Table 8. Root-Mean-Square Deviation (RMSD), Mean-Signed Error (MSE), Mean-Unsigned Error (MUE), and Maximum Error (MAX) on the MGAE109 Database in kcal mol^{-1} for Unmodified MP2, Attenuated MP2, VV10-Corrected Attenuated MP2, and Spin-Component Scaled VV10-Corrected Attenuated MP2

method	RMSD	MSE	MUE	MAX
MP2/aTZ	9.04	−1.83	7.38	23.31
SCS-MP2/aTZ	7.78	−5.98	6.27	24.15
MP2(terfc, aTZ)	9.38	−2.97	7.57	23.48
SCS-MP2(2terfc, aTZ)	5.15	−2.12	3.68	21.79
MP2-V(terfc, aTZ)	11.07	−5.64	9.13	24.63
SCS-MP2-V(2terfc, aTZ)	5.20	−2.70	3.69	22.16

Table 9. Root-Mean-Square Deviation (RMSD), Mean-Signed Error (MSE), Mean-Unsigned Error (MUE), and Maximum Error (MAX) on the G2/97 Database in kcal mol^{-1} for Unmodified MP2, Attenuated MP2, VV10-Corrected Attenuated MP2, and Spin-Component Scaled VV10-Corrected Attenuated MP2

method	RMSD	MSE	MUE	MAX
MP2/aTZ	8.28	−0.52	6.68	23.72
SCS-MP2/aTZ	6.17	−4.41	5.03	23.32
MP2(terfc, aTZ)	8.37	−1.80	6.74	23.97
SCS-MP2(2terfc, aTZ)	5.35	0.61	3.79	20.97
MP2-V(terfc, aTZ)	9.69	−4.71	7.99	25.16
SCS-MP2-V(2terfc, aTZ)	5.15	−1.69	3.54	21.46

For the G2/97 database, MP2-V(terfc, aTZ) also performs poorly (with an RMSD of 9.69 kcal mol^{-1}). The poor performance of MP2-V(terfc, aTZ) underscores the fact that it cannot be recommended for evaluation of bonded interactions. As in the MGAE109 database, SCS-MP2-V(2terfc, aTZ) performs very well on the G2/97 database with an RMSD of 5.15 kcal mol^{-1}, surprisingly almost 1 kcal mol^{-1} lower than SCS-MP2/aTZ and almost 3 kcal mol^{-1} lower than MP2/aTZ. We conclude that the spin-component scaled model exhibits quite satisfactory transferability for bonded interactions, although its performance is not on par with leading density functionals.

5. CONCLUSIONS

This work paired attenuated MP2 with long-range VV10 dispersion correction within the aug-cc-pVTZ basis set with spin-component scaling also used to improve short-range bonded interactions. From training on the W4-11 and S66 databases, we see shorter-range attenuation parameters relative to uncorrected attenuated MP2, as well as useful reductions in RMS errors for not only our training sets but also our test sets. For nonbonded interactions, we believe this results from the

DOI: 10.1021/acs.jctc.5b00509
J. Chem. Theory Comput. 2015, 11, 4159−4168

improved physical content in van der Waals corrected attenuated MP2. Our recommendations for use are as follows:

1. For noncovalent interactions, the MP2-V(2terfc, aTZ) and SCS-MP2-V(2terfc, aTZ) methods are an improvement over the original attenuated method, MP2(terfc, aTZ), for all classes of noncovalent interactions and have correct asymptotic treatment of van der Waals interactions. In a statistical sense, these methods typically outperform MP2/aTZ and even complete basis set MP2. Like MP2, these methods are self-interaction free, which is an advantage relative to present-day DFT.

2. For thermochemistry, the SCS-MP2-V(2terfc, aTZ) method consistently performs as well as SCS-MP2/aTZ or better while incorporating more appropriate long-range physics. As such, we recommend this method for modeling bond-breaking reactions in complex chemical environments, particularly when it is important to be self-interaction free.

3. When incorporating the long-range van der Waals correction, attenuated MP2 includes only quite short-ranged MP2 correlation, as evidenced by the smaller attenuation parameters. Not only is the physical content improved, but because MP2-V(terfc, aTZ) is even shorter-ranged in the MP2 correlation, there is potential for a lower prefactor in a specialized algorithm. This is a problem that deserves future attention.

■ ASSOCIATED CONTENT

Supporting Information

The Supporting Information is available free of charge on the ACS Publications website at DOI: 10.1021/acs.jctc.5b00509.

Breakdown of error metrics for S66 interaction types, binding energies for the stretched dimers of Figures 5−7 and for the S66x8, S66a8, and A21 × 12 databases, and geometries for the A21 × 12 database stretched dimers (PDF)

Geometries for argon-methane dimer (ZIP)

Geometries for ethene dimer (ZIP)

Geometries for water dimer (ZIP)

Geometries for A21 × 12 (ZIP)

■ AUTHOR INFORMATION

Corresponding Author

*E-mail: mhg@cchem.berkeley.edu.

Present Addresses

[¶]M.B.G.: Institute for Molecular Engineering, The University of Chicago, Chicago, Illinois 60637, United States

[§]B.B.: Université de Toulouse, UPS, IRSAMC, Laboratoire de Chimie et Physique Quantiques, CNRS (UMR 5626), 118 Route de Narbonne, F-31062, Toulouse, France

Notes

The authors declare the following competing financial interest(s): M.H.G. is a part-owner of Q-Chem Incorporated.

■ ACKNOWLEDGMENTS

This work was supported by the U.S. Department of Energy under Contract No. DE-AC02-05CH11231 with additional support from Q-Chem Incorporated through NIH SBIR Grant No. GM096678. We acknowledge computational resources obtained under NSF award CHE-1048789. M.H.G. is part-owner of Q-Chem Incorporated.

■ REFERENCES

(1) Pople, J. A. *Angew. Chem., Int. Ed.* **1999**, *38*, 1894−1902.
(2) Møller, C.; Plesset, M. S. *Phys. Rev.* **1934**, *46*, 618−622.
(3) Cremer, D. *WIREs Comput. Mol. Sci.* **2011**, *1*, 509−530.
(4) Yoo, S.; Apra, E.; Zeng, X. C.; Xantheas, S. S. *J. Phys. Chem. Lett.* **2010**, *1*, 3122−3127.
(5) Temelso, B.; Archer, K. A.; Shields, G. C. *J. Phys. Chem. A* **2011**, *115*, 12034−12046.
(6) Mardirossian, N.; Lambrecht, D. S.; McCaslin, L.; Xantheas, S. S.; Head-Gordon, M. *J. Chem. Theory Comput.* **2013**, *9*, 1368−1380.
(7) Lao, K. U.; Schaffer, R.; Jansen, G.; Herbert, J. M. *J. Chem. Theory Comput.* **2015**, *11*, 2473.
(8) Jurecka, P.; Sponer, J.; Cerny, J.; Hobza, P. *Phys. Chem. Chem. Phys.* **2006**, *8*, 1985−1993.
(9) Jung, Y.; Head-Gordon, M. *Phys. Chem. Chem. Phys.* **2006**, *8*, 2831−2840.
(10) Cybulski, S. M.; Lytle, M. L. *J. Chem. Phys.* **2007**, *127*, 141102.
(11) Janowski, T.; Pulay, P. *J. Am. Chem. Soc.* **2012**, *134*, 17520−17525.
(12) Szabo, A.; Ostlund, N. S. *J. Chem. Phys.* **1977**, *67*, 4351−4360.
(13) Tkatchenko, A.; DiStasio, R. A., Jr.; Head-Gordon, M.; Scheffler, M. *J. Chem. Phys.* **2009**, *131*, 094106.
(14) Helgaker, T.; Klopper, W.; Koch, H.; Noga, J. *J. Chem. Phys.* **1997**, *106*, 9639−9646.
(15) Van Mourik, T. *J. Phys. Chem. A* **2008**, *112*, 11017−11020.
(16) Gordon, M.; Truhlar, D. *J. Am. Chem. Soc.* **1986**, *108*, 5412−5419.
(17) Fast, P. L.; Corchado, J.; Sanchez, M. L.; Truhlar, D. G. *J. Phys. Chem. A* **1999**, *103*, 3139−3143.
(18) Grimme, S. *J. Chem. Phys.* **2003**, *118*, 9095−9102.
(19) Antony, J.; Grimme, S. *J. Phys. Chem. A* **2007**, *111*, 4862−4868.
(20) DiStasio, R. A., Jr.; Head-Gordon, M. *Mol. Phys.* **2007**, *105*, 1073−1083.
(21) Gerenkamp, M.; Grimme, S. *Chem. Phys. Lett.* **2004**, *392*, 229−235.
(22) Goumans, T. P. M.; Ehlers, A. W.; Lammertsma, K.; Wurthwein, E. U.; Grimme, S. *Chem. - Eur. J.* **2004**, *10*, 6468−6475.
(23) Hyla-Kryspin, I.; Grimme, S. *Organometallics* **2004**, *23*, 5581−5592.
(24) Grimme, S. *J. Phys. Chem. A* **2005**, *109*, 3067−3077.
(25) van Mourik, T.; Gdanitz, R. J. *J. Chem. Phys.* **2002**, *116*, 9620−9623.
(26) Grimme, S. *J. Comput. Chem.* **2004**, *25*, 1463−1473.
(27) Grimme, S. *J. Comput. Chem.* **2006**, *27*, 1787−1799.
(28) Chai, J.; Head-Gordon, M. *Phys. Chem. Chem. Phys.* **2008**, *10*, 6615−6620.
(29) Grimme, S.; Antony, J.; Ehrlich, S.; Krieg, H. *J. Chem. Phys.* **2010**, *132*, 154104.
(30) Becke, A. D.; Johnson, E. R. *J. Chem. Phys.* **2007**, *127*, 154108.
(31) Tkatchenko, A.; Scheffler, M. *Phys. Rev. Lett.* **2009**, *102*, 073005.
(32) Vydrov, O.; Wu, Q.; Van Voorhis, T. *J. Chem. Phys.* **2008**, *129*, 014106.
(33) Vydrov, O.; Van Voorhis, T. *Phys. Rev. Lett.* **2009**, *103*, 7−10.
(34) Vydrov, O.; Van Voorhis, T. *J. Chem. Phys.* **2010**, *133*, 244103.
(35) Vydrov, O.; Van Voorhis, T. *Phys. Rev. A: At., Mol., Opt. Phys.* **2010**, *81*, 1−6.
(36) Vydrov, O.; Van Voorhis, T. *J. Chem. Theory Comput.* **2012**, *8*, 1929−1934.
(37) Mardirossian, N.; Head-Gordon, M. *Phys. Chem. Chem. Phys.* **2014**, *16*, 9904−9924.
(38) Mardirossian, N.; Head-Gordon, M. *J. Chem. Phys.* **2015**, *142*, 074111.
(39) Grafenstein, J.; Kraka, E.; Cremer, D. *J. Chem. Phys.* **2004**, *120*, 524−539.
(40) Cohen, A. J.; Mori-Sanchez, P.; Yang, W. T. *Chem. Rev.* **2012**, *112*, 289−320.
(41) Goldey, M.; Head-Gordon, M. *J. Phys. Chem. Lett.* **2012**, *3*, 3592−3598.

DOI: 10.1021/acs.jctc.5b00509
J. Chem. Theory Comput. 2015, 11, 4159−4168

(42) Goldey, M.; Dutoi, A.; Head-Gordon, M. *Phys. Chem. Chem. Phys.* **2013**, *15*, 15869−15875.
(43) Dunning, T. H., Jr. *J. Chem. Phys.* **1989**, *90*, 1007−1023.
(44) Kendall, R. A.; Dunning, T. H., Jr. *J. Chem. Phys.* **1992**, *96*, 6796.
(45) Goldey, M. B.; Head-Gordon, M. *Chem. Phys. Lett.* **2014**, *608*, 249−254.
(46) Goldey, M.; DiStasio, R. A., Jr.; Shao, Y.; Head-Gordon, M. *Mol. Phys.* **2014**, *112*, 836−843.
(47) Goldey, M.; Head-Gordon, M. *J. Phys. Chem. B* **2014**, *118*, 6519−6525.
(48) Huang, Y.; Goldey, M.; Head-Gordon, M.; Beran, G. *J. Chem. Theory Comput.* **2014**, *10*, 2054−2063.
(49) Huang, Y.; Shao, Y.; Beran, G. J. O. *J. Chem. Phys.* **2013**, *138*, 224112.
(50) Thirman, J.; Head-Gordon, M. *J. Phys. Chem. Lett.* **2014**, *5*, 1380−1385.
(51) Dutoi, A. D.; Head-Gordon, M. *J. Phys. Chem. A* **2008**, *112*, 2110−2119.
(52) Řezáč, J.; Riley, K. E.; Hobza, P. *J. Chem. Theory Comput.* **2011**, *7*, 2427−2438.
(53) Shao, Y.; Gan, Z.; Epifanovsky, E.; Gilbert, A. T. B.; Wormit, M.; Kussmann, J.; Lange, A. W.; Behn, A.; Deng, J.; Feng, X.; Ghosh, D.; Goldey, M.; Horn, P. R.; Jacobson, L. D.; Kaliman, I.; Khaliullin, R. Z.; Kuś, T.; Landau, A.; Liu, J.; Proynov, E. I.; Rhee, Y. M.; Richard, R. M.; Rohrdanz, M. A.; Steele, R. P.; Sundstrom, E. J.; Woodcock, H. L.; Zimmerman, P. M.; Zuev, D.; Albrecht, B.; Alguire, E.; Austin, B.; Beran, G. J. O.; Bernard, Y. A.; Berquist, E.; Brandhorst, K.; Bravaya, K. B.; Brown, S. T.; Casanova, D.; Chang, C.-M.; Chen, Y.; Chien, S. H.; Closser, K. D.; Crittenden, D. L.; Diedenhofen, M.; DiStasio, R. A.; Do, H.; Dutoi, A. D.; Edgar, R. G.; Fatehi, S.; Fusti-Molnar, L.; Ghysels, A.; Golubeva-Zadorozhnaya, A.; Gomes, J.; Hanson-Heine, M. W. D.; Harbach, P. H. P.; Hauser, A. W.; Hohenstein, E. G.; Holden, Z. C.; Jagau, T.-C.; Ji, H.; Kaduk, B.; Khistyaev, K.; Kim, J.; Kim, J.; King, R. A.; Klunzinger, P.; Kosenkov, D.; Kowalczyk, T.; Krauter, C. M.; Lao, K. U.; Laurent, A. D.; Lawler, K. V.; Levchenko, S. V.; Lin, C. Y.; Liu, F.; Livshits, E.; Lochan, R. C.; Luenser, A.; Manohar, P.; Manzer, S. F.; Mao, S.-P.; Mardirossian, N.; Marenich, A. V.; Maurer, S. A.; Mayhall, N. J.; Neuscamman, E.; Oana, C. M.; Olivares-Amaya, R.; ONeill, D. P.; Parkhill, J. A.; Perrine, T. M.; Peverati, R.; Prociuk, A.; Rehn, D. R.; Rosta, E.; Russ, N. J.; Sharada, S. M.; Sharma, S.; Small, D. W.; Sodt, A.; Stein, T.; Stück, D.; Su, Y.-C.; Thom, A. J. W.; Tsuchimochi, T.; Vanovschi, V.; Vogt, L.; Vydrov, O.; Wang, T.; Watson, M. A.; Wenzel, J.; White, A.; Williams, C. F.; Yang, J.; Yeganeh, S.; Yost, S. R.; You, Z.-Q.; Zhang, I. Y.; Zhang, X.; Zhao, Y.; Brooks, B. R.; Chan, G. K. L.; Chipman, D. M.; Cramer, C. J.; Goddard, W. A.; Gordon, M. S.; Hehre, W. J.; Klamt, A.; Schaefer, H. F.; Schmidt, M. W.; Sherrill, C. D.; Truhlar, D. G.; Warshel, A.; Xu, X.; Aspuru-Guzik, A.; Baer, R.; Bell, A. T.; Besley, N. A.; Chai, J.-D.; Dreuw, A.; Dunietz, B. D.; Furlani, T. R.; Gwaltney, S. R.; Hsu, C.-P.; Jung, Y.; Kong, J.; Lambrecht, D. S.; Liang, W.; Ochsenfeld, C.; Rassolov, V. A.; Slipchenko, L. V.; Subotnik, J. E.; Van Voorhis, T.; Herbert, J. M.; Krylov, A. I.; Gill, P. M. W.; Head-Gordon, M. *Mol. Phys.* **2015**, *113*, 184−215.
(54) Weigend, F.; Köhn, A.; Hättig, C. *J. Chem. Phys.* **2002**, *116*, 3175−3183.
(55) Karton, A.; Daon, S.; Martin, J. M. *Chem. Phys. Lett.* **2011**, *510*, 165−178.
(56) Rezáč, J.; Riley, K. E.; Hobza, P. *J. Chem. Theory Comput.* **2011**, *7*, 3466−3470.
(57) Goerigk, L.; Grimme, S. *Phys. Chem. Chem. Phys.* **2011**, *13*, 6670−6688.
(58) Marshall, M. S.; Burns, L. A.; Sherrill, C. D. *J. Chem. Phys.* **2011**, *135*, 194102.
(59) Rezáč, J.; Hobza, P. *J. Chem. Theory Comput.* **2013**, *9*, 2151−2155.
(60) Witte, J.; Goldey, M.; Neaton, J. B.; Head-Gordon, M. *J. Chem. Theory Comput.* **2015**, *11*, 1481−1492.
(61) Steele, R. P.; DiStasio, R. A., Jr.; Head-Gordon, M. *J. Chem. Theory Comput.* **2009**, *5*, 1560−1572.
(62) Steele, R. P.; DiStasio, R. A., Jr.; Shao, Y.; Kong, J.; Head-Gordon, M. *J. Chem. Phys.* **2006**, *125*, 074108.
(63) Peverati, R.; Truhlar, D. G. *J. Chem. Phys.* **2011**, *135*, 191102.
(64) Haunschild, R.; Klopper, W. *J. Chem. Phys.* **2012**, *136*, 164102.

DOI: 10.1021/acs.jctc.5b00509
J. Chem. Theory Comput. 2015, 11, 4159−4168